

de Haas–van Alphen measurements in the ferromagnetic compounds U_3P_4 and U_3As_4

Z. Henkie

*Institute for Low Temperature and Structural Research, Polish Academy of Sciences, PL-50-950 Wroclaw, Poland*W. R. Johanson,* A. J. Arko, and G. W. Crabtree
Argonne National Laboratory, Argonne, Illinois 60439

C. Bazan

International Laboratory for High Magnetic Fields and Low Temperatures, PL-50-520 Wroclaw, Poland

(Received 14 March 1983)

de Haas–van Alphen measurements are reported for the ferromagnetic actinide compounds U_3P_4 and U_3As_4 . The large effective masses indicate f -electron interaction with conduction bands. The data are interpreted in terms of a semimetallic band structure producing a large electron sheet at point Γ which is compensated by several smaller hole pockets along the Γ – P line. The measured internal field is much smaller than expected on the basis of magnetization measurements. Several discrepancies with other measurements point to additional unobserved pieces of the Fermi surface.

INTRODUCTION

The degree of itinerancy of the $5f$ electrons in actinide compounds is one of the more important parameters determining the magnetic, electronic, and transport properties in these materials. To date, de Haas–van Alphen (dHvA) measurements have been reported in systems where f electrons are totally itinerant,¹ forming a strong d – f or p – f bond, and also in systems where f electrons are purely localized² ($5f^2$ configuration in UPd_3) but nonmagnetic. In this paper we present the first dHvA study of the Fermi surface in a magnetically ordered actinide compound. Effective-mass data (see below) strongly suggest that while f electrons form magnetic moments in this system, in all likelihood they also hybridize with the conduction states. Thus U_3P_4 and U_3As_4 represent an intermediate state between localization and itinerancy.

U_3P_4 and U_3As_4 crystallize in the Th_3P_4 -type bcc structure³ with two formula units per unit cell. They are ferromagnetic below 138 and 198 K, respectively,^{4–8} and show unusually large magnetic,^{9–12} magnetostriction,¹⁰ and resistivity¹³ anisotropy with respect to $\langle 111 \rangle$, the direction of spontaneous magnetization. The saturation moment along this easy magnetic direction in U_3As_4 is $1.8\mu_B/U$ atom,¹⁴ corresponding to an internal field $4\pi M_{\text{sat}} = 4.2$ kOe. In U_3P_4 , the $\langle 111 \rangle$ saturation moment is $1.2\mu_B/U$ atom,¹⁵ giving an internal field $4\pi M_{\text{sat}} = 3.1$ kOe. More recent work⁸ essentially confirms these saturation values.

The magnetic moments on the uranium atom sites do not actually orient⁸ along $\langle 111 \rangle$. Indeed the magnetic structure consists of an unusual, noncollinear, three sublattice configuration where the six spins in each unit cell pair up and actually align approximately along the three $\langle 112 \rangle$ directions surrounding the $\langle 111 \rangle$ easy magnetization direction of each magnetic domain. While the spins will tilt somewhat in a large magnetic field, a field of 300

kOe is insufficient to saturate¹⁵ either material along $\langle 100 \rangle$. It was suggested by Kasuya and co-workers¹⁶ that the same anisotropic mixing mechanism between f states and valence electrons used to explain the anisotropic behavior of cerium monopnictides may be applicable in the interpretation of the anisotropy in uranium compounds.

Without participation of $5f$ electrons in the conduction bands it would be difficult to explain the metallic behavior of U_3P_4 and U_3As_4 . The corresponding thorium compounds (Th_3P_4 and Th_3As_4) have the same crystal structure³ and are diamagnetic semiconductors^{17–19} with indirect energy gaps of 0.40 and 0.43 eV, respectively. Positron annihilation experiments,²⁰ which point to a corelike behavior for f electrons in the uranium compounds, indicate that the same number of valence electrons are involved in bonding in both Th and U compounds. Optical reflectivity data²¹ are similar except shifted by approximately 0.8 eV as the energy gap is closed and the semiconductor becomes a compensated semimetal. (The compensation is to be expected on the basis of the even number of electrons per unit cell, and is consistent with the low positive value of the Hall²² constant as well as the magnetoresistivity^{23,24} results.) The $5f$ electrons are the most likely candidates to fill the gap, probably via p – f hybridization. This would help explain the extremely sensitive effect of pressure on the electrical resistivity²⁵ and the relatively small magnetic moments compared to the free uranium atom.

The present dHvA study was undertaken to investigate some of the above speculations. Since the dHvA effect is sensitive to conduction electrons only, it is possible to obtain direct, detailed information on the free carriers. An accompanying band-structure calculation would of course be quite valuable for extending the picture of the electronic structure derived from our experiment. It would be helpful, for example, to determine whether the itinerant f character is due to direct f – f overlap, f – d overlap, or to

f - p overlap from neighboring phosphorus sites. Perhaps the present work will stimulate such a calculation.

EXPERIMENTAL DETAILS

Many lanthanide and actinide compounds which crystallize in the Th_3P_4 -type structure show a wide range of composition (up to 2:3 stoichiometry). Fortunately, the thorium and uranium pnictides are not in this group. Faceted crystals of excellent quality (up to 0.5 cm on a side) can be grown by chemical-vapor transport.^{25,26} Several U_3P_4 crystals with resistance ratios ranging from 300 to 550 and several U_3As_4 crystals with resistance ratios of about 400 were selected from a large number grown by this process. They were first spark cut into a cube typically 1.5 mm on a side, and then ground into a sphere of approximately 1 mm diam. in a rotating alumina crucible containing the etchant $H_2O/HCl/HNO_3$ (ratios 1:2:1 and 4:2:1 for U_3P_4 and U_3As_4 , respectively). Spherical samples are necessary in ferromagnetic materials, since the internal \vec{B} field can then be calculated [$=\vec{B}_a + (8\pi/3)\vec{M}$, where \vec{B}_a is the applied field and \vec{M} is the magnetization] and is uniform throughout the sample. The orientation of crystals in the sample holder was determined to within 2° by standard x-ray and optical techniques.²⁷ In the case of U_3As_4 the signal was sufficiently strong to enable the use of the dHvA effect itself for orientation via a rotation diagram shown in Fig. 1.

Data were taken in the (110) plane in fields up to 150 kOe in the (0.3–0.8)-K temperature range (pumped 3He), utilizing the usual field-modulation technique.²⁷ The data were digitized and Fourier-analyzed with an on-line computer. It was generally not necessary to correct for the internal field (see below).

RESULTS AND DISCUSSION

The extremal cross-sectional areas (in a.u.) obtained both for U_3P_4 and U_3As_4 in the (110) plane are shown in Fig. 2. (For those preferring frequency units, 0.04 a.u. = 15×10^6 G.) Effective masses were measured for several field directions and are indicated (value and direction) on the figure. The Dingle temperature was measured in U_3P_4 at the same angle as m^* and found to be $T_D = 0.05$. This number is surprisingly low considering the relatively low value of the resistance ratio. However, the resistance ratio was measured at 4.2 K where spin-

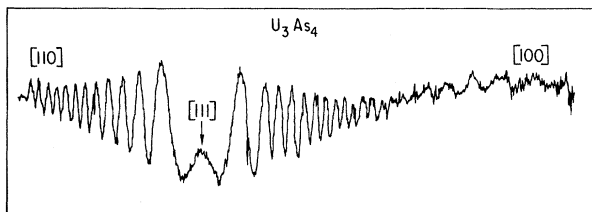


FIG. 1. Rotation diagram showing dHvA oscillations in U_3As_4 as a function of applied field direction at constant field strength.

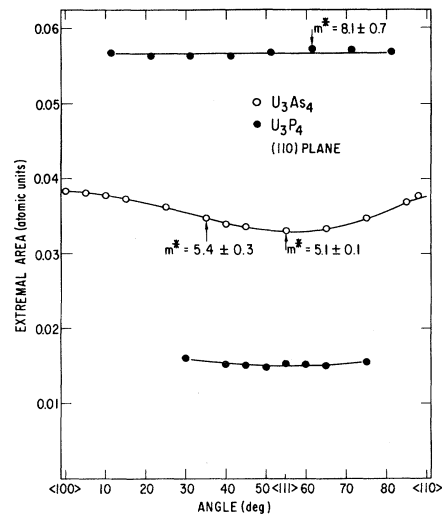


FIG. 2. Observed cross-sectional areas for the Fermi surfaces of U_3As_4 and U_3P_4 as a function of field direction in the (110) plane. Arrows indicate the angles at which effective-mass measurements were made, with the results shown.

disorder resistivity (proportional to T^2) constitutes²³ a sizable fraction of the total resistivity. This means in effect that the crystals are far more perfect than one would gather simply from the 4.2-K resistance ratio.

A single branch is observed in U_3As_4 , corresponding to a single closed sheet with an area anisotropy of approximately 16%. The signal is strongest for $\vec{H} \parallel \langle 111 \rangle$ (the easy magnetization direction) as is evident from the rotation diagram of Fig. 1, but it is observed in the entire (110) plane except precisely at [110]. The decrease in signal strength is faster than would be expected from the increase in effective mass (5.1 to 5.4 in 20°), and is probably associated with multidomain formation¹³ as the field direction approaches either $\langle 110 \rangle$ or $\langle 100 \rangle$ where any one of three $\langle 111 \rangle$ -type axes are equally preferred for \vec{M} . Indeed it is surprising that the signal could be observed over such a large angular range. Because of multidomain formation, we could not take data in the (100) plane where a unique $\langle 111 \rangle$ axis for \vec{M} does not exist.

Two branches were observed for U_3P_4 , neither of which could be followed to $\langle 100 \rangle$ or $\langle 110 \rangle$, most likely for the above reasons, but also because of the fact that m^*/m_0 for the larger sheet was approximately 8.1, a 60% increase over U_3As_4 . The m^* for the smaller branch could not be measured because of experimental difficulties inherent in the field-modulation technique for small, heavy-mass frequencies. The larger m^* as well as the larger Fermi-surface extremal area in U_3P_4 vs U_3As_4 would seem to indicate a greater interaction of $5f$ electrons with conduction electrons in U_3P_4 , a fact consistent with the neutron⁸ and saturation moment^{14,15} results which show a smaller moment on the U site in U_3P_4 . A smaller anisotropy energy in U_3P_4 would also allow easier multidomain formation as \vec{H} approaches $\langle 100 \rangle$ or $\langle 110 \rangle$. In any case, we believe that both branches observed in U_3P_4 correspond to closed

surfaces, in which case their volume difference is a factor of 7.3 if both sheets are assumed to be spherical. This suggests a Fermi surface (shown in Fig. 3) which consists of a nearly spherical, heavy-mass electron sheet centered at point Γ , and eight smaller, nearly spherical hole pockets somewhere along the Γ - P line in the bcc Brillouin zone, which exactly compensate the hole sheet. This semimetallic Fermi surface can explain the low positive value²² of the Hall constant and the positive thermopower²² as being due to high mobility holes on the small sheets. The "semiconducting-type" critical behavior in the resistivity²² at the Curie point can also be understood since our model is closely related to the indirect gap semiconducting band structure of Th_3P_4 . It does not, however, agree well with the optical reflectivity data²¹ and the angular variation of the magnetoresistance,²³ as we will see below.

A smaller sheet of Fermi surface is not observed in U_3As_4 , but the similarities in the properties between the two materials strongly suggests that it should be there. Magnetoresistivity data²³ show that U_3As_4 is also compensated so that the total volume of the electron pockets equals the hole volume. If we again have eight hole pockets, then an orbit about half the size of the small U_3P_4 orbit is needed for compensation, i.e., approximately 0.008 a.u. (or 3×10^6 G). Since the m^*/m_0 of this small orbit is again likely to be greater than 1, it would be very difficult to observe with field modulation which in our case is limited to 400 G peak to peak.

Band-structure calculations to test the plausibility of our Fermi-surface model are not yet available for U_3P_4 and U_3As_4 . These materials have rather complicated structures which do not contain a center of inversion symmetry, making their band structures difficult to calculate.

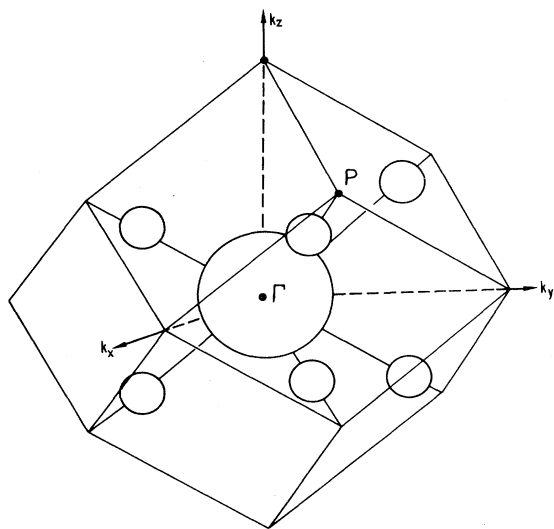


FIG. 3. Schematic model of the Fermi surfaces of U_3As_4 and U_3P_4 . Large, nearly spherical electron sheet at point Γ is compensated by eight smaller, nearly spherical hole sheets located along with Γ - P line. Electron and hole sheets are observed in U_3P_4 ; only the electron sheet is observed in U_3As_4 .

However, there is one recent band calculation²⁸ for the isostructural semiconductor Th_3P_4 , which shows a conduction-band minimum at point Γ and valence-band maxima along the Γ - H lines, at point H , and along the Γ - N lines. A semimetallic band structure can be derived from the Th_3P_4 bands most simply by rigidly raising the valence bands and lowering the conduction bands, creating an electron pocket at point Γ and hole pockets at the valence-band maxima. All sheets of this Fermi surface would be closed. If only one of the three valence-band maxima overlaps the conduction band, a hole pocket with a volume ratio to the electron sheet of 1/6 would be observed for holes along the Γ - H line, 1/12 for holes along the Γ - N line, and 1/3 for holes at the H point. None of these values agree with our estimated volume ratio of 1/7.3 as well as our proposed Fermi-surface model with holes along the Γ - P line and a volume ratio of 1/8. It is possible to make our observations consistent with a rigid shift of the Th_3P_4 bands by assuming that more than one type of compensating hole sheet is present, but only one type is observed. However, it seems likely that the $5f$ electrons of U will significantly alter the crystal potential, especially since the existence of magnetic order in the U compounds implies these electrons have predominantly local character. In this case, a rigid shift of the conduction bands relative to the valence bands is too simple a description. Rather, one expects the individual bands to be affected in different ways, including both rigid shifts in energy and distortion of the $E(\vec{k})$ dispersion. Therefore a correct interpretation of our Fermi-surface measurements in terms of a band structure must await a detailed treatment of the $5f$ states in U_3As_4 and U_3P_4 .

One proposal for making such a detailed calculation relies on the p - f -mixing hypothesis introduced^{16,29} to explain the strong magnetic anisotropy in CeSb and CeBi. As applied to U_3As_4 and U_3P_4 , this proposal places the U $5f^2$ levels well below the Fermi level and assumes a strong interaction between the f states and the valence-band p states.^{28,30} This p - f mixing shifts the valence p states up in energy until they overlap the conduction band, creating valence-band holes and conduction-band electrons. The energy of this p - f mixing is an important contribution to the total energy of the system, and contributes to the magnetic anisotropy by maintaining the $5f$ levels in orientations most favorable to a strong p - f interaction. Because the transfer of electrons from the valence to the conduction band is a fundamental feature of this model, Fermi-surface measurements provide an important test of its validity. Our estimates of the volume ratios for the two sheets we observe indicate that the two most likely places for valence-band holes are along the Γ - P line and Γ - H line.

A second approach to the electronic structure of magnetic Ce and U compounds is based on the anisotropic two-ion-interaction model.³¹ In this model, first proposed for Ce compounds³² (f^1) and later generalized to U compounds³³ (f^2 and f^3), anisotropy with respect to the U-U direction is caused by a small amount of hybridization of the mostly ionic f electrons with the conduction band. It is capable of explaining³³ the noncollinear magnetic structure of UAs, and may also be applicable to

U₃As₄ and U₃P₄. However, there has not yet been any discussion of the effect of this hybridization mechanism on the Fermi surface, so no comparison with our experimental results is possible.

In U₃As₄ we measured the effective internal saturation field H_{eff} by making a linear fit of the oscillation number to $1/B$ where $B = H_{\text{appl}} + H_{\text{eff}}$. For spherical samples it is anticipated¹⁴ that $H_{\text{eff}} = 8\pi/3M_{\text{sat}} = 2.8$ kOe in U₃As₄. In the plot (shown in Fig. 4), H_{eff} is an adjustable parameter which is varied to force the straight-line fit. The best fit was obtained for $H_{\text{eff}} = 0.75$ kG, a number much lower than the expected 2.8 kG. (The parameter Δ is an arbitrary zero offset for the n th oscillation and can be ignored.) The dashed line in the figure shows the fit for $H_{\text{eff}} = 0$ and indicates a clear upward curvature. The curvature is reversed downward for $H_{\text{eff}} = 2.8$ kG. We do not understand the reasons for this large discrepancy but we suspect it may be related to the unusual noncollinear magnetic structure. In any case, our measured $H_{\text{eff}} \ll H_{\text{appl}}$, so that errors obtained by ignoring H_{eff} in the determination of the dHvA frequencies in Fig. 2 are never more than 4% in U₃As₄. For U₃P₄ the corrections would seem to be even smaller than in U₃As₄ based on the line shapes of the Fourier-transform peaks of the data, which are very sensitive to any nonlinear effects. In this case also then, H_{eff} was ignored in calculating frequencies.

Assuming no ferromagnetic splitting of the bands (i.e., again ignoring H_{eff}), the volume of the single observed sheet in U₃As₄ corresponds to 0.043 carriers/formula unit (0.014 carriers/U atom) and that of the large sheet in U₃P₄ to 0.078 carriers/formula unit or 0.026 carriers/U atom. If we double this amount to account for the hole pockets we will obtain only 0.052 carriers/U atom in U₃P₄. Optical reflectivity measurements,²¹ on the other hand, suggest a conduction-electron concentration of 0.5 per U atom. Such a large discrepancy would seem to be beyond experimental error even after accounting for all the approximations of the Drude fit, and strongly suggests that there may be additional pieces of Fermi surface as yet unobserved. If band splitting is present the discrepancy

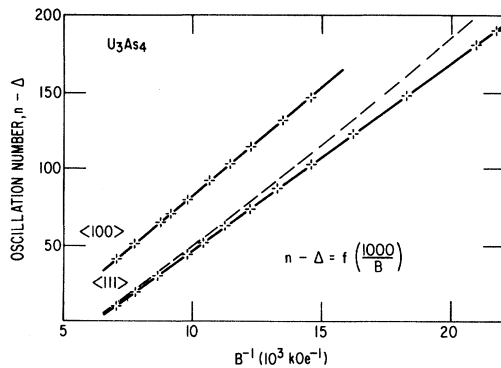


FIG. 4. Number plot for U₃As₄ in the $\langle 100 \rangle$ and $\langle 111 \rangle$ directions. Data were fit to the expression $n - \Delta = f/B$, where $B = H_{\text{appl}} + H_{\text{eff}}$. Best fit was obtained for $H_{\text{eff}} = 0.75$ kG, shown as the solid line. Crosses are the data for this value of H_{eff} . For $\langle 111 \rangle$, dashed line shows the trend of the data for $H_{\text{eff}} = 0$.

becomes even larger.

Magnetoresistance data²³ indicate the existence of open orbits perpendicular to the $\langle 100 \rangle$ directions. If such orbits exist, they are not reflected in the small pieces of surface we report here, and indicate the existence of an additional multiply connected sheet of the Fermi surface. If the closed orbits supported by this sheet occur along $\langle 100 \rangle$ or $\langle 110 \rangle$ we may not see them, because for fields near these directions the sample breaks into magnetic domains with the magnetization along equivalent $\langle 111 \rangle$ directions. These domains tend to destroy the spatial coherence of the sample and diminish the amplitudes of the dHvA oscillations, rendering them difficult to observe. Hence, the existence of open orbits on an additional sheet of the Fermi surface is not inconsistent with the dHvA data presented here.

An important test of our Fermi-surface model can be made using electronic specific-heat measurements. These experiments provide information about the many-body-enhanced electronic density of states at the Fermi level, a quantity closely related to the cyclotron effective mass. The nearly spherical sheets of the Fermi surface in our model may be treated in the isotropic approximation in order to estimate the density of states from the measured cross-sectional areas and cyclotron effective masses. For a single spherical sheet, the density of states is given by

$$n(E) = 4(a/2\pi)^3(m^*/\hbar^2)\sqrt{\pi A},$$

where $n(E)$ is the density of states/unit energy unit cell spin, a the lattice constant of the unit cell, and m^* and A the measured effective mass and cross-sectional area, respectively. This relation is valid for an isotropic Fermi surface formed by an energy band of arbitrary curvature. For the large sheet of U₃As₄, the measured values of m^* and A imply a density of states of 1.1 states/eV formula unit spin (corresponding to an electronic specific heat $\gamma = 5.0$ mJ/K² mole formula unit), and for U₃P₄, 1.9 states/eV formula unit spin (corresponding to $\gamma = 9.0$ mJ/K² mole formula unit). Since we have no mass measurements on the small sheets we cannot estimate their contribution to the density of states as reliably as for the large sheets. However, we expect the mass of the small sheet to be less than that of the large sheet, and for our purposes we may project the value of the mass by either of two assumptions: (1) That the curvature of the energy bands forming the small sheet is the same as that of the large sheet, or (2) that the Fermi velocity of the two sheets is the same. In the first case the mass scales with the area of the orbit, and each small sheet contributes $\frac{1}{4}$ of the density of states of the large sheet. In the second case the mass scales with circumference of the orbit, and each small sheet contributes $\frac{1}{8}$ of that of the large sheet. Since there are eight small sheets, their total density of states is either twice that of the large sheet or equal to that of the large sheet, depending on which assumption is made. Thus for U₃P₄ our estimates for γ are 18 and 27 mJ/mole K² while for U₃As₄ they are 10 and 15 mJ/mole K². Although these estimates are necessarily imprecise, they give the order of magnitude for the electronic specific heat expected on the basis of our Fermi-surface

model. If other sheets of the Fermi surface exist, these estimates provide a lower limit to the electronic specific heat.

The available experimental measurements of the electronic specific heats of U_3As_4 and U_3P_4 are in strong disagreement with each other.³⁴ This disagreement is partly due to the difficulty of separating the large magnetization contribution from the phonon contribution to the specific heat, and partly due to the lack of data at temperatures low enough for reliable extrapolation to $T=0$. For U_3P_4 a value of $\gamma=76.5$ mJ/mole formula unit K^2 was reported by Counsell *et al.*³⁵ from data taken above 11 K, while Stalinsky *et al.*³⁶ did not attempt to determine γ from their data taken above 22.5 K. For U_3As_4 , there are measurements of 3.76 mJ/mole formula unit K^2 by Alles *et al.*³⁷ from data taken above 5 K, and 66.0 mJ/mole formula unit K^2 by Mortimer.³⁸ In view of the wide range of the experimental results it is difficult to conclude anything from comparisons with our model predictions.

In summation, then, our dHvA data are consistent with a compensated semimetallic Fermi surface for both U_3As_4

and U_3P_4 . The large values of m^* indicate an interaction of f electrons with conduction electrons. The interaction would appear to be stronger in U_3P_4 than in U_3As_4 which is consistent with the smaller moment observed in neutron and magnetization measurements in U_3P_4 . The measured internal field in U_3As_4 is much smaller than anticipated from saturation magnetization measurements, a discrepancy we do not understand. The open orbits indicated by magnetoresistance data and the larger number of carriers derived from optical reflectivity data suggest the existence of an additional sheet to the Fermi surface. While we see no evidence of this sheet, it is not necessarily inconsistent with our results. Our model predicts values for the enhanced density of electronic states at the Fermi level and for the electronic specific heat, but the scatter in the specific-heat measurements which have been reported prevents a conclusive experimental test of our prediction.

ACKNOWLEDGMENTS

This work was supported by the U.S. Department of Energy.

*Present address: Pomona College, Pomona, CA 91711.

¹A. J. Arko and J. E. Schirber, *J. Phys. (Paris) Colloq.* **40**, C4-9 (1979), and references therein.

²A. van Deursen (unpublished).

³R. N. Wycköff, in *Crystal Structures* (Interscience, New York, 1964), Vol. 2, p. 100.

⁴C. F. Buhner, *J. Phys. Chem. Solids* **30**, 1273 (1969).

⁵R. Troć, J. Mulak, and W. Suski, *Phys. Status Solidi B* **43**, 147 (1971).

⁶J. Przystawa, *J. Phys. Chem. Solids* **31**, 2158 (1970).

⁷J. Przystawa and E. Praveczi, *J. Phys. Chem. Solids* **33**, 1943 (1972).

⁸P. Burelt, J. Rossat-Mignond, R. Troć, and Z. Henkie, *Solid State Commun.* **39**, 745 (1981).

⁹W. Trzebiatowski, Z. Henkie, K. P. Bielov, A. S. Dimitrievsky, R. Z. Levitin, and Yu. P. Popov, *Zh. Eksp. Teor. Fiz.* **61**, 1522 (1971).

¹⁰K. P. Bielov, Z. Henkie, A. S. Dimitrievsky, R. Z. Levitin, and W. Trzebiatowski, *Zh. Eksp. Teor. Fiz.* **64**, 1351 (1973).

¹¹V. E. Brili, R. Z. Levitin, R. E. Osipowa, V. L. Yakovenko, and M. Zelený, *Phys. Status Solidi A* **57**, 393 (1980).

¹²R. Troć, J. Sznajd, P. Novotny, and T. Mydlarz (unpublished).

¹³Z. Henkie, *Physica* **102B**, 329 (1980).

¹⁴R. Troć, J. Sznajd, P. Novotny, and T. Mydlarz, *J. Magn. Mater.* **23**, 129 (1981).

¹⁵K. P. Bielov, Z. Henkie, A. S. Dimitrievskii, A. Zygmunt, P. Z. Levitin, and Yu. P. Popov, in *Proceedings of the International Conference on Magnetism, ICM-73* (Nauka, Moscow, 1974), Vol. 4, p. 54.

¹⁶K. Takegahara, A. Yanase, and T. Kasuya, *J. Phys. (Paris) Colloq.* **41**, C5-327 (1980).

¹⁷F. L. Carter, in *Rare Earth Research III*, edited by L. Eyring (Gordon and Breach, New York, 1965), p. 495.

¹⁸Z. Henkie, P. J. Markowski and E. Zdanowicz, in *Proceedings*

of the 2nd International Conference on Electronic Structure of the Actinides, edited by J. Mulak, W. Suski, and R. Troć (Ossolineum, Wroclaw, 1977), p. 425.

¹⁹Z. Henkie and P. J. Markowski, *J. Phys. Chem. Solids* **39**, 39 (1978).

²⁰B. Rozenfeld, E. Denbowska, and Z. Henkie, *J. Solid State Chem.* **17**, 101 (1976).

²¹J. Schoenes, private communication.

²²Z. Henkie, *Bull. Acad. Polon. Sci., Ser. Sci.-Chim.* **20**, 531 (1972).

²³C. Bazan, Z. Henkie, and Z. Pawłowska, in *Proceedings of the 2nd International Conference on Electronic Structure of the Actinides*, Ref. 18, p. 431.

²⁴C. Bazan, private communication.

²⁵Z. Henkie, *Phys. Status Solidi A* **58**, K219 (1980); *Z. Henkie, Roczniki Chemii* **42**, 363 (1968).

²⁶Z. Henkie and P. J. Markowski, *J. Cryst. Growth* **41**, 303 (1977).

²⁷R. W. Stark and L. R. Windmiller, *Cryogenics* **8**, 272 (1968).

²⁸T. Suzuki, S. Takagi, N. Niitsuma, K. Takegahara, T. Kasuya, A. Yanase, T. Sakakibara, M. Date, P. J. Markowski, and Z. Henkie, in *Proceedings of the International Symposium on High Field Magnetism, Osaka, 1982*, edited by M. Date (North-Holland, Amsterdam, in press).

²⁹K. Takegahara, H. Takahashi, A. Yanase, and T. Kasuya, *J. Phys. C* **14**, 737 (1981).

³⁰K. Takegahara, A. Yanase, and T. Kasuya, in *Crystalline Electric Fields and f Electron Magnetism*, edited by R. P. Guertin, W. Suski, and Z. Zolnierrek (Plenum, New York, 1982), p. 533.

³¹B. Coqblin and J. R. Schrieffer, *Phys. Rev.* **185**, 847 (1969).

³²R. Siemann and B. R. Cooper, *Phys. Rev. Lett.* **44**, 1015 (1980).

³³B. R. Cooper, P. Thayamballi, and O. Vogt, *J. Magn. Magn.*

- Mater. 31-34, 235 (1983); P. Thayamballi and B. R. Cooper, J. Appl. Phys. (in press).
- ³⁴A. Blaise, J. Phys. (Paris) Colloq. 40, C4 (1979).
- ³⁵J. F. Counsell, R. M. Dell, A. R. Junkinson, and J. F. Martin, Trans. Faraday Soc. 63, 72 (1967).
- ³⁶B. Stalinsky, Z. Bieganski, and R. Troć, Phys. Status Solidi 17, 837 (1966).
- ³⁷A. Alles, B. G. Falk, E. F. Westrum, Jr., F. Grönvold, and M. R. Zaki, J. Inorg. Nucl. Chem. 39, 1993 (1977).
- ³⁸M. J. Mortimer, Atomic Energy Research Establishment (Harwell, United Kingdom) Report No. R8852, 1977 (unpublished).